

Strong azimuthal anchoring energy at a nematic-polyimide interface

S. Faetti* and P. Marianelli

INFM and Dipartimento di Fisica, Università di Pisa, Largo Pontecorvo 3, 56127 Pisa, Italy

(Received 1 August 2005; published 14 November 2005)

Some years ago we proposed an automated reflectometric method to measure the director azimuthal angle at the interface between a nematic liquid crystal and another medium. The method ensures a great accuracy and sensitivity and is virtually unaffected by the presence of a director bulk distortion. This latter property makes it possible to measure strong anchoring energies. In the present experiment, we use this method to measure the azimuthal anchoring energy at the interface between the nematic liquid crystal 4-pentyl-4'-cyanobiphenyl (5CB) and a rubbed polyimide layer. This kind of interface is characterized by a strong azimuthal anchoring and, thus, it represents a good test for the proposed reflectometric method. An ac planar electric field is applied to a nematic layer and the consequent azimuthal rotation of the director at the interface is measured. The anchoring energy coefficient W_a at room temperature is strong ($W_a=0.33 \times 10^{-3} \text{ J/m}^2$) and decreases greatly as the clearing temperature is approached. The time response of the azimuthal surface director angle to a stepwise electric field evidences the characteristic slow dynamics which is currently observed for weak anchoring substrates.

DOI: 10.1103/PhysRevE.72.051708

PACS number(s): 61.30.Hn

I. INTRODUCTION

Interfacial phenomena in nematic liquid crystals (NLC) are object of a lot of attention both for their relevance to basic physics and for the applications in the optoelectronic industry. Nematic liquid crystals are usually sandwiched between two plane transparent solid plates that determine the resulting orientation of the average long molecular axis denoted by the unit vector $\mathbf{n}(\mathbf{r})$ (the *director*) [1]. The director orientation at the interface is characterized by the zenithal angle θ_s with the normal z -axis and the azimuthal angle ϕ_s with a x axis on the surface plane. The alignment of the surface director \mathbf{n}_s is determined by the competition between surface and bulk interactions. In the absence of external torques, the director is aligned along the *easy axis* \mathbf{n}_e which minimizes the surface anchoring energy $W(\mathbf{n}_s)$ [1,2]. $W(\mathbf{n}_s)$ represents the work which is needed to rotate the director from the easy axis \mathbf{n}_e toward the actual surface orientation \mathbf{n}_s . The anchoring at the interfaces plays an important role on the macroscopic behavior of nematic liquid crystals. Indeed, the bulk director field, the threshold fields and the dynamic behavior of NLC are greatly affected by the anchoring energy. If θ_s is held fixed and equal to the easy polar angle θ_e , $W(\theta_s, \phi_s)$ becomes a function of ϕ_s only and is called the *azimuthal anchoring energy*. If the director remains close to the easy axis, the azimuthal anchoring energy is well represented by the parabolic form:

$$W = \frac{W_a}{2} (\phi_s - \phi_e)^2, \quad (1)$$

where W_a is a coefficient named azimuthal anchoring energy coefficient and which measures the strength of the azimuthal anchoring.

The azimuthal anchoring energy can be measured applying an azimuthal external torque on the director and measuring the consequent change of the surface azimuthal angle. The external torque can be generated either applying external fields (magnetic, electric) or exploiting the competition between different surface orientations (hybrid cell). Different experimental methods have been proposed to measure the azimuthal surface director rotation. Most of them consist on the optical measurement of the polarization state of either transmitted [3–11] or reflected [12–19] light. All these methods provide accurate measurements of weak azimuthal anchoring energies ($W_a \ll 10^{-4} \text{ J/m}^2$), but most of them are not appropriate to measure strong anchoring energies ($W_a > 10^{-4} \text{ J/m}^2$). Indeed, the measurement of strong anchoring energies needs the application of high external torques on the nematic sample to produce an appreciable surface director rotation. These torques induce a rotation of the director at the surface but also an interfacial director twist with a small characteristic length which affects the polarization state of the transmitted and the reflected light. This noisy effect is especially relevant for the transmission light methods and leads to spurious optical signals that simulate great apparent surface rotations. For strong anchoring, the apparent surface rotations can be some orders of magnitude higher than the true surface director rotation.

In a recent paper [15] we proposed an automated reflectometric method which provides high sensitivity and high accuracy and is virtually insensitive to the specific optical characteristics of the interface. Furthermore, with the choice of a special geometry, the reflectometric method is virtually unaffected by the presence of the bulk director twist also in the high external fields regime. Therefore, strong azimuthal anchoring energies can be measured accurately with this method.

The interface between a nematic liquid crystal and a rubbed polyimide substrate is currently used both in experimental investigations of liquid crystals and in display indus-

*Author to whom correspondence should be addressed. Email address: faetti@df.unipi.it

try. This interface is known to be chemically stable and to induce a strong azimuthal anchoring [10]. Therefore, this kind of interface represents a good test for our reflectometric method. In this paper we report measurements of the azimuthal anchoring energy between the nematic liquid crystal 5CB and a substrate of rubbed polyimide. The azimuthal anchoring energy is measured as a function of the temperature. We find a strong azimuthal anchoring at room temperature characterized by the anchoring coefficient $W_a = 0.33 \times 10^{-3} \text{ J/m}^2$ which corresponds to the small extrapolation length [1] $d_e = 12 \text{ nm}$. The anchoring energy greatly decreases as the temperature approaches the clearing temperature $T_c = 35 \text{ }^\circ\text{C}$. The dynamic response of the surface azimuthal angle to a step-wise planar electric field is characterized by a first fast response (time scale lower than a few seconds) followed by a very slow drift (time scale greater than many minutes and hours). A similar slow drift has been often reported in the literature in the case of weak anchoring and has been explained in terms of a gliding of the easy axis [13,19–26]. Note that also a gliding of the surface zenithal angle has been recently reported for the interface between 5CB and the same rubbed polyimide used for the present experiment [27]. From these experimental results we infer that the gliding phenomenon is not a peculiar feature of weak anchoring but is a very general property which characterizes the interfacial interactions between a nematic liquid crystal and a different medium. In Sec. II, we shortly describe the experimental apparatus and the nematic cell and the experimental procedure used to measure the spatial dependence of the electric field. In Sec. III, the experimental measurements of the anchoring energy are reported together with the evidence for the easy axis gliding. Section IV is devoted to conclusions.

II. EXPERIMENTAL PROCEDURES

A. The wedge cell and the experimental apparatus

The details of the reflectometric method have been discussed extensively in Ref. [15], then here we only summarize the main points. The method exploits the anisotropy of the reflection coefficients at the interface between a nematic liquid crystal and an isotropic medium.

Figure 1 shows schematically the experimental apparatus. A monochromatic laser beam (He-Ne, $\lambda = 632.8 \text{ nm}$) passes through a polarizer P , a basculating compensator C and a mirror M_1 . Then, this beam passes through a polarizer P_1 which rotates with the constant angular velocity $\omega = 5.71 \text{ rad/s}$. The polarizer P and the basculating compensator C are set in such a way to produce a circular polarization of the optical beam reflected by mirror M_1 . For an elliptic polarization, the intensity of the beam transmitted by the rotating polarizer P_1 is a sinusoidal function with pulsation 2ω . The oscillation amplitude vanishes for a circularly polarized wave. In our experiment, we set the optical compensator C in order to reduce the residual modulation amplitude at the pulsation 2ω much lower than 0.5%. Note that, also in these conditions, a 4% modulation at the pulsation ω is always present in the experiment due to some spurious contribution caused by the non-ideality of the rotating polar-

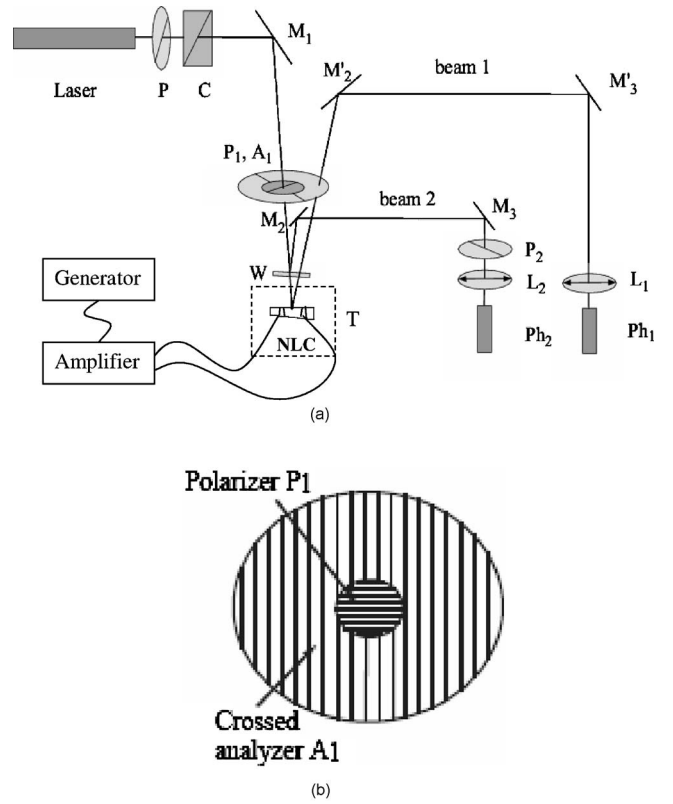


FIG. 1. (a) Experimental reflectometric apparatus. P and P_i ($i=1,2$)=polarizers, C =tilting optical compensator, M_i ($i=1,2,3$) and M'_i ($i=2,3$), W =wedge glass plate (wedge angle of 1°), L_i ($i=1,2$)=lenses, Ph_i ($i=1,2$)=photodiodes, NLC=wedge cell with the NLC, and T =thermostatic box. The system P_1 - A_1 represents two concentric crossed polarizers glued together and rotating at a constant angular velocity. (b) Detail of the system of the crossed rotating polarizers P_1 - A_1 . The polarizers are made by two crossed concentric polaroids glued together on the border line.

izer P_1 . However, according to the analysis reported below, this latter modulation does not appreciably affect the accuracy of the anchoring energy measurements. The beam transmitted by polarizer P_1 impinges at nearly normal incidence (within 1°) on a nematic wedge cell inserted in a thermostatic box that ensures a temperature accuracy and stability better than $0.1 \text{ }^\circ\text{C}$. The beam reflected by the nematic-polyimide interface passes through analyzer A_1 which is crossed with respect to polarizer P_1 and rotates solidally with it. Then the beam is focused on photodiode Ph_1 . A reference beam is obtained by inserting an isotropic wedge glass plate W between the polarizer P_1 and the nematic cell. The beam reflected by the glass plate passes through a fixed polarizer P_2 and is focused on photodiode Ph_2 . The output of photodiode Ph_2 is a cosinusoidal signal at the angular frequency 2ω with a phase which can be set at any value by changing the orientation of polarizer P_2 . This signal provides a phase-reference signal in our experiment. According to Ref. [15], the intensity of the reflected laser beam which impinges on photodiode Ph_1 is

$$I'(t) = I_o b_0 [a_0 - \cos 4(\omega t - \phi_s - \phi_{app})], \quad (2)$$

where I_o is the intensity of the incident beam, b_0 is a suitable reflectivity coefficient, a_0 is an adimensional coefficient

($a_0 \approx 1$), ϕ_s is the surface director azimuthal angle and ϕ_{app} is an apparent rotation due to the presence of the bulk director twist. It has been shown that this apparent rotation is very small also for relatively strong interfacial twist distortions. Furthermore, it is further reduced if the director at the surface is close to 90° with respect to the external orienting field (magnetic or electric). In the present experiment we use an electric field which makes an angle of 85° with the surface easy axis. At the maximum electric field ($E=0.4 \text{ V}/\mu\text{m}$), the apparent rotation is $\phi_{app} < 0.002^\circ$ which is completely negligible with respect to the true surface director rotation which is of the order of one degree. Then, the oscillating signal in Eq. (2) is reduced to

$$I'(t) = I_o b_0 [a_0 - \cos 4(\omega t - \phi_s)]. \quad (3)$$

The surface azimuthal angle ϕ_s can be simply obtained from the measurement of the phase of the reflected intensity I' in Eq. (3). Note that this measurement does not require the knowledge of the bulk constants of the NLC and any fitting procedure. These features make the reflectometric method very simple, accurate and direct. The outputs of the two photodiodes Ph_1 and Ph_2 are sent to a PC computer which makes the Fourier transform of the two signals at the angular frequencies 2ω and 4ω calculating amplitudes and phases of both signals.

The cell containing the NLC [see Figs. 2(a) and 2(b)] is made by two plane glass plates separated by two brass stripes of different thicknesses ($d_1=50 \mu\text{m}$ and $d_2=100 \mu\text{m}$) that produce a wedge with angle $\Delta\theta \approx 1.6^\circ$. The internal glass surfaces of the cell are covered by a thin film of polyimide (Nissan Corporation SE-3510) which has been rubbed with a velvet roll along a given axis in the plane of the layer. The rubbing is unidirectional and done a single time (one passage). The rubbed polyimide plates were supplied by S. Joly of Nemoptic. An important parameter which characterizes the strength of rubbing is the total length L of the rubbing cloth which contacts a certain point of the substrate. This parameter depends on the number N of cumulative rubs ($N=1$), on the contact width l of velvet on the glass plate ($l=2 \times 10^{-2} \text{ m}$), on the number n of revolutions of the velvet roll ($n=500 \text{ rpm}$) on the radius r of the velvet roll ($r=4.75 \times 10^{-2} \text{ m}$) and on the translation velocity v of the substrate stage ($v=10^{-2} \text{ m/s}$). Using the theoretical expression of L given in Eq. (2) of Ref. [28], we find $L \approx 5 \text{ m}$. This treatment gives a strong anchoring with the pretilt angle $\theta_p \approx 6^\circ$.

The wedge shape of the cell makes possible to separate spatially the different beams that are reflected by the two glasses and to select the ones coming from the first glass (air-glass reflected beam and glass-polyimide reflected beam). The beam reflected by the isotropic air-glass interface of the first glass has the same polarization of the incident beam and, thus, is stopped by the crossed analyzer A_1 . Then, only the beam reflected by the anisotropic polyimide-nematic interface can pass through the rotating analyzer A_1 . The NLC used in this experiment is 4-pentyl-4'-cyanobiphenyl (5CB) purchased by Merck and having the clearing temperature $T_c=35^\circ \text{C}$. The NLC is inserted by capillarity in the cell under vacuum to avoid the formation of air bubbles. The two

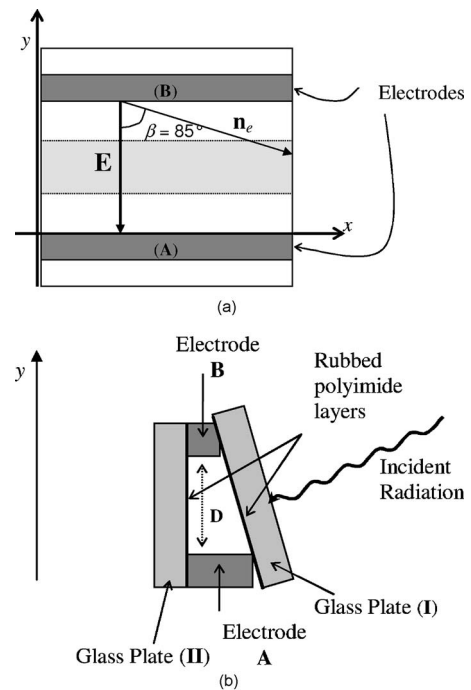


FIG. 2. Schematic top (a) and side (b) views of the wedge cell containing the NLC. The two figures are not in scale. Glass I and glass II are two plane glasses, whilst A and B are two brass stripes of different thicknesses at distance $D=1.78 \text{ mm}$. The internal surfaces of the glasses are covered by a thin rubbed polyimide layer. An ac voltage V , applied between the two electrodes, generates an electric field \mathbf{E} along the y axis which makes the angle $\beta=85^\circ$ with respect to the rubbing direction of polyimide. The light grey stripe shown in (a) represents the region of the cell where the electric field is virtually uniform and equal to $E=0.90 \text{ V}/D$.

brass stripes make an angle of about 5° with the rubbing axis and their distance is $D=1.78 \text{ mm}$. An ac voltage at the 500 Hz frequency with the maximum value of 700 V rms can be applied between the two stripes to produce an electric field at 85° with respect to the rubbing direction. The voltage amplifier used to generate the high voltage electric field provides two simultaneous voltage outputs V_1 and $V_2=-V_1$ (symmetrical with respect to ground) which are connected to the two conducting stripes of the cell. This kind of electrical connection minimizes the space inhomogeneities of the electric field.

B. The electric field spatial distribution and the measurement method

For strong anchoring energies, appreciable surface director rotations can be only obtained by applying sufficiently strong external azimuthal torques. For this reason, in this experiment we use an electric field instead of a magnetic field. Indeed, our maximum electric field (rms value $E=0.4 \text{ V}/\mu\text{m}$) is equivalent to a magnetic induction field of about 4 T . Furthermore, the use of an electric field allows us to avoid spurious signals due to the Faraday rotation in the glass windows of the thermostatic box and in those of the nematic cell. This spurious rotation is negligible for weak

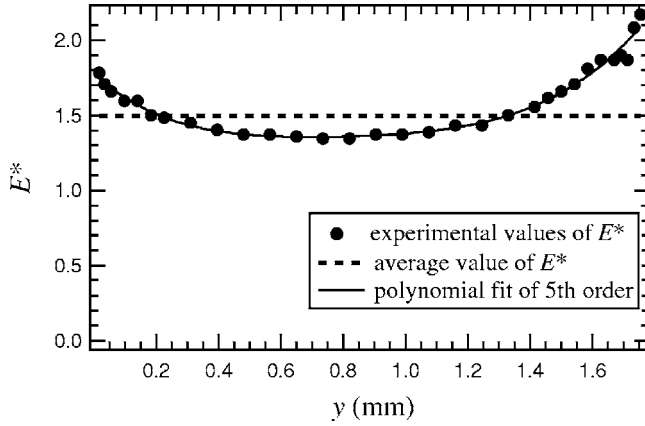


FIG. 3. Dependence of E^* on the y distance from the thicker electrode. Full points represent the measured values of the adimensional parameter $E^* = [\tan(\Delta\phi_c)]^{-1/2}$, where $\Delta\phi_c$ is the measured dephasing. The full line represents the best fit with a fifth-order polynomial, whilst the broken line represents the average value of E^* . The rms average value of the applied voltage is $V=218$ V and the modulation frequency is $\omega_m=18.8$ rad/s.

anchoring but could be not completely negligible in the case of very strong anchoring.

A drawback of the use of the planar electric field is that this field is not uniform and its precise spatial behavior is not known. For this reason we have performed a preliminary measurement in order to determine the space variation of the electric field between the two electrodes and to localize the regions of the cell where the electric field is sufficiently uniform. The experimental method exploits the proportionality of the response time of the director field to E^{-2} [1] (the electric field is much greater than the Fredericksz threshold). In this experiment, we use a polarizing microscope to obtain an enlarged image of the nematic sample between the two electrodes using white light. The sample is observed between crossed polarizers and is rotated until the extinction position is reached where the NLC appears dark. Then, an electric field much higher than the Fredericksz threshold is switched on and the NLC becomes bright due to the presence of a strong director twist. The light outcoming from a small circular area of the NLC (0.05 mm diameter) is focused on a photodiode. The output of the photodiode is connected to the input of a lock-in amplifier. Then the ac electric field is modulated at a low frequency with modulation amplitude lower than 10%. In these conditions, the output of the photodiode oscillates at the modulation frequency with a dephasing $\Delta\phi_c$ which is due to the finite response time of the twist distortion. Before starting the measurements, we have verified experimentally that $\tan(\Delta\phi_c)$ is proportional to E^{-2} , where E is the average rms value of the modulated electric field. Therefore, the parameter $E^* = [\tan(\Delta\phi_c)]^{-1/2}$ in different points between the electrodes satisfies the simple condition $E = \alpha E^*$, where α is a suitable multiplicative coefficient.

Full points in Fig. 3 are the experimental values of E^* at different distances from the thicker electrode. We see that the electric field increases greatly close to the two electrodes and reaches a virtually constant value in a central region of the cell at distances between 0.5 mm and 0.9 mm from the

thicker electrode. The broken line in Fig. 3 represents the space average value of E^* . From Fig. 3 we see that the ratio between the value of E^* at the center of the cell and the average value is 0.90. Then, the electric field at the center of the cell can be obtained using the simple expression $E = 0.9 V/D$ where V is the difference of potential between the electrodes and D is the distance between the electrodes. All the following measurements of surface director angles reported in this paper have been performed using a laser beam which impinges in this region of the sample where the electric field is virtually uniform (light gray stripe in Fig. 2). The diameter of the laser beam spot on the nematic cell is ≈ 0.25 mm.

In order to measure the azimuthal anchoring energy, we use the procedure below.

(1) Without an applied electric field, we measure the phase ϕ_1 of the 4ω component of the signal and the phase ϕ_2 of the 2ω component of the reference signal. Then, the computer calculates the parameter $\delta\phi = \phi_1/4 - \phi_2/2$. Rotating polarizer P_2 on the reference beam, we set $\delta\phi = 0$ degrees.

(2) We switch on the electric field (much greater than the Fredericksz threshold) and we measure the variation $\Delta\delta\phi$ of $\delta\phi$ after the short director relaxation time (< 1 s). According to Eq. (3), the azimuthal rotation $\Delta\phi_s$ of the director at the surface is just given by $\Delta\delta\phi$.

(3) The anchoring energy coefficient is, then, obtained using the simple expression (see Ref. [13]):

$$W_a = \frac{\sqrt{K_{22}\epsilon_a\epsilon_0} E \sin(\beta)}{\Delta\phi_s}, \quad (4)$$

where K_{22} is the twist elastic constant of 5CB, ϵ_a is its dielectric anisotropy, ϵ_0 is the vacuum dielectric constant, E is the rms value of the ac electric field, $\beta = 85^\circ$ is the azimuthal angle between the easy axis and the electric field and $\Delta\phi_s$ represents here the absolute value of the surface director rotation.

Equation (4) holds for electric fields much higher than the threshold field and for small surface rotations. For higher surface director rotations, the parabolic approximation of the anchoring energy in Eq. (1) has to be replaced by the well known Rapini-Papoular expression [1] and W_a is obtained using the equation

$$W_a = \frac{2\sqrt{K_{22}\epsilon_a\epsilon_0} E \sin(\beta - \Delta\phi_s)}{\sin(2\Delta\phi_s)}, \quad (5)$$

which reduces to Eq. (4) for $\Delta\phi_s \ll 1$ rad.

III. EXPERIMENTAL RESULTS

A. Experimental sources of noise and preliminary results

For strong anchoring energies, the surface rotations induced by strong external torques are somewhat small and, thus, a special care must be devoted to avoid spurious signals that can simulate apparent surface rotations. Furthermore, the intensity of the beam reflected by the nematic-polyimide interface is very small and, thus, the diffused light which impinges on the photodiode can trouble the experimental re-

sults. Another source of errors (probably the most important) is related to the rotating polarizers. In our experiment, the rotating crossed polarizers P_1 and A_1 are made by two circular concentric polaroid plates that are glued together with the polarizing axes at 90° [see Fig. 1(b)]. During the rotation of the polarizers, the reflected beam passes through different points of the analyzer [see Fig. 1(a)]. Therefore, possible inhomogeneities of the extinction ratio of the polaroids can produce a spurious modulation of the measured signal that can affect the phase measurement. In our opinion this is actually the most important source of systematic noise in the experiment. This spurious modulation is probably responsible for a 2ω component of the reflected intensity at zero applied field which is always observed in the experiment together with the expected 4ω -component. For this reason, polaroids that ensure high and homogeneous extinction ratios ($>0.5 \times 10^4$) everywhere have been carefully selected. This choice leads to a great reduction of the amplitude of the 2ω component. One other possible source of errors is due to the presence of a residual birefringence of glasses and of the rubbed polyimide orienting layer. Indeed, it is known [29] that the rubbed polyimide shows a small birefringence (the typical optical dephasing between extraordinary and ordinary beam is $\approx 1^\circ$). The order of magnitude of the systematic error induced by this birefringence on the measurement of the surface director rotation can be estimated by measuring the oscillation amplitude A_0 of the reflected intensity $I'(t)$ after the rotating analyzer A_1 . For a NLC in the isotropic phase in the contact with an isotropic substrate, this amplitude should be zero whilst it is different from zero if some small birefringence of the substrate occurs. In order to avoid pretransitional effects due to the residual nematic order at the interfaces, the measurements in the isotropic phase have to be done at a temperature well above the clearing value ($T - T_c > 1^\circ\text{C}$). It has been shown [15] that the ratio between the amplitudes $I_o(\text{isotropic})$ and $I_o(\text{nematic})$ measured when the NLC is, respectively, well above and below the clearing temperature represents a good estimate of the relative error on the director surface rotation due to the residual birefringence of the substrate.

Figure 4 shows the experimental amplitude A_0 of the oscillating signal [$I_o b_0$ in Eq. (3)] for different temperatures. This amplitude decreases as the temperature approaches the clearing value and becomes close to zero for $T - T_c \approx 2^\circ\text{C}$. The ratio $A_o(\text{isotropic})/A_o(\text{nematic})$ remains below 0.01 in the whole nematic range. Then, according to the theoretical results in Ref. [15], we can conclude that this error source leads to a relative uncertainty on the measurement of the surface director rotation lower than 1% in our experimental conditions.

The oscillation amplitude A_0 of the intensity of the reflected beam for isotropic polyimide is expected to be proportional to

$$R = \left[\frac{n_p - n_o}{n_p + n_o} - \frac{n_p - n(\theta_p)}{n_p + n(\theta_p)} \right]^2, \quad (6)$$

where n_o is the ordinary refractive index of the NLC, n_p is the refractive index of polyimide, θ_p is the pretilt angle and

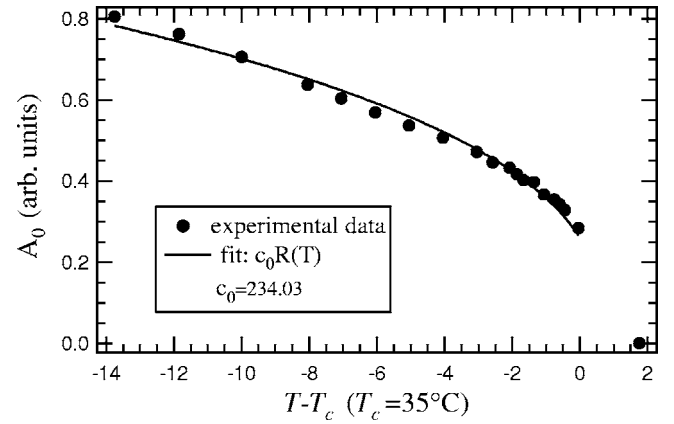


FIG. 4. Full points represent the measured oscillation amplitude A_0 of the intensity of the reflected beam for different values of the temperature T . T_c is the clearing temperature of the NLC. The oscillation amplitude is nearly vanishing above the clearing temperature (point at $T - T_c \approx 2^\circ\text{C}$). The full line represents the best fit with the function $y = c_0 R(T)$ where c_0 is a free coefficient and $R(T)$ is the function defined in Eq. (6).

$n(\theta_p)$ is the refractive index seen by the extraordinary wave which is given by [30]

$$\frac{1}{n(\theta_p)^2} = \frac{\cos^2(\theta_p)}{n_e^2} + \frac{\sin^2(\theta_p)}{n_o^2}, \quad (7)$$

where n_e is the extraordinary refractive index of the NLC. Using the experimental data of the refractive indices of 5CB [31] together with the parameters $n_p = 1.7$ and $\theta_p = 6^\circ$, we find that R in Eq. (6) is satisfactorily fitted by the simple analytical expression $R(T) = 0.00126(0.707 - T_r)^{0.365}$, where T_r is the reduced temperature ($T_r = T - T_c$). The full line in Fig. 4 represents the best fit of the experimental oscillation amplitudes A_o with the function $y = c_0 R(T)$, where c_0 is the only free fitting coefficient ($c_0 = 234$). Although it is evident the presence of small systematic deviations (of the order of 3%), the satisfactory agreement between experiment and theory suggests that error sources as those due to light diffusion from the NLC or to inhomogeneities of the rotating polarizers are not relevant in our experimental conditions.

Another important test of reliability of the measurements consists on measuring the surface director rotation $\Delta\phi_s$ induced by the switching on of the electric field in different points of the NLC sample. For a uniformly rubbed polyimide, a constant value of $\Delta\phi_s$ is expected. According to our previous experience, space variations of $\Delta\phi_s$ are often evidence for the presence of spurious noise contributions. Figure 5 shows the surface rotation which is measured at the switching on of the electric field in different points along the x axis parallel to the electrodes in the central region of the NLC where the electric field is virtually uniform [see Fig. 2(a)]. Within the random experimental noise, the surface rotation is the same everywhere. Finally, the elastic theory predicts that the surface rotation angle must be proportional to the rms value of the applied electric field E [see Eq. (4)] if it is much higher than the Freedericksz threshold field E_c ($E_c < 0.01 \text{ V}/\mu\text{m}$ in our experimental conditions). This theoret-

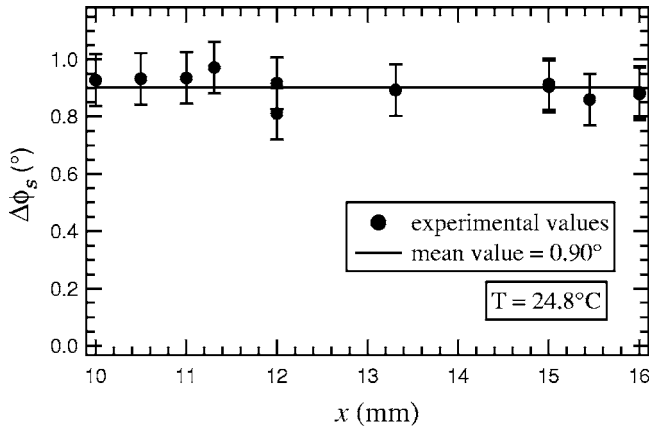


FIG. 5. Surface azimuthal rotation $\Delta\phi_s$ of the director due to the switching on of an electric field with rms value $E=0.24 \text{ V}/\mu\text{m}$. Full points represent the rotation angle in different points of the cell along the x axis parallel to the electrodes. All these measurements have been performed in the central region between the electrodes where the electric field is nearly uniform. The horizontal full line represents the average value of $\Delta\phi_s$. The temperature of the sample is $T=24.8^\circ\text{C}$. The error bars correspond to two standard deviations.

ical prediction is well satisfied by the experimental results shown in Fig. 6. Note that many spurious sources of noise as well as, for instance, the Kerr effect in the glass plates and the small mechanical deformations of the glass plates produced by the electric field depend on the square power of the electric field. Therefore, the linearity of our experimental results demonstrates that these sources of systematic errors are negligible in our experiment.

B. Measurements of azimuthal anchoring energy

Figure 7 shows the director surface rotation $\Delta\phi_s$ versus temperature when an electric field with rms value

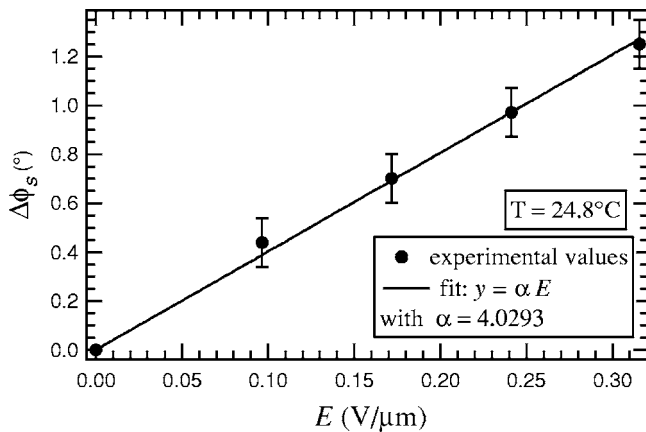


FIG. 6. Surface azimuthal rotation $\Delta\phi_s$ of the director due to the switching on of an electric field versus the rms value E of the applied ac field. Full points represent the experimental results. The full line corresponds to the best fit with the theoretical linear function $y=\alpha E$. The temperature of the sample is $T=24.8^\circ\text{C}$. The error bars correspond to two standard deviations.

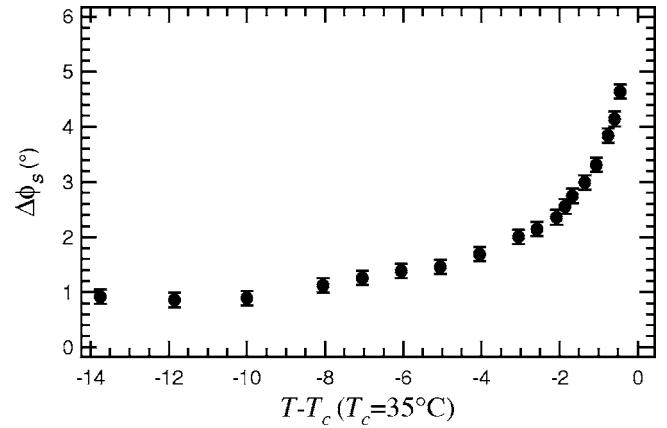


FIG. 7. Surface azimuthal rotation $\Delta\phi_s$ of the director due to the switching on of an electric field versus the reduced temperature $T_r=T-T_c$. The rms value of the electric field is $E=0.24 \text{ V}/\mu\text{m}$. The error bars correspond to two standard deviations.

$E=0.24 \text{ V}/\mu\text{m}$ is switched on. It is evident that $\Delta\phi_s$ increases greatly as the temperature approaches the clearing value. Substituting in Eq. (4) the experimental values of the elastic constant K_{22} [32] and of the dielectric anisotropy [33] together with the experimental values of E , β and $\Delta\phi_s$, we obtain the anchoring energy shown in Fig. 8(a) and the corresponding extrapolation length $d_e=K_{22}/W_a$ shown in Fig. 8(b).

It is evident from these experimental results that the anchoring energy at room temperature is very strong ($W_a=0.33 \times 10^{-3} \text{ J}/\text{m}^2=0.33 \text{ erg}/\text{cm}^2$) and the extrapolation length is small ($d_e=12 \text{ nm}$). This anchoring energy is about ten times the one which has been measured with obliquely evaporated SiO at 60° [13] and many orders of magnitude higher than those that are usually measured in the literature on other kinds of substrates [3,4,9,19]. The anchoring energy reduces greatly while approaching the clearing temperature. Note that the extrapolation length in Fig. 8(b) shows an appreciable increase whilst increasing the temperature. We remind that the extrapolation length d_e is defined by $d_e=K_{22}/W_a$, where K_{22} is the twist elastic constant which is virtually proportional to the square power of the scalar order parameter S [1]. Then, the increase of d_e with the temperature means that the anchoring energy coefficient decreases with the temperature much more rapidly than S^2 . An analogous decrease of the anchoring energy while approaching the clearing temperature has been often observed for weak [19] and moderately strong anchoring [13]. In order to have an indirect confirm of these experimental results we have also performed some measurements of the azimuthal anchoring energy using a different experimental method with transmitted light which was recently proposed by one of us [11]. Due to the use of the wedge geometry, with this method we avoid the interference effects between extraordinary and ordinary beams that greatly affect the accuracy of the standard transmitted light methods [5]. In this experiment, we use the same laser beam which impinges on the nematic wedge cell in Fig. 1 but we detect the transmitted ordinary (or extraordinary) beam instead of the reflected one. Due to the wedge shape of the cell, the incident laser beam is separated into an ordinary

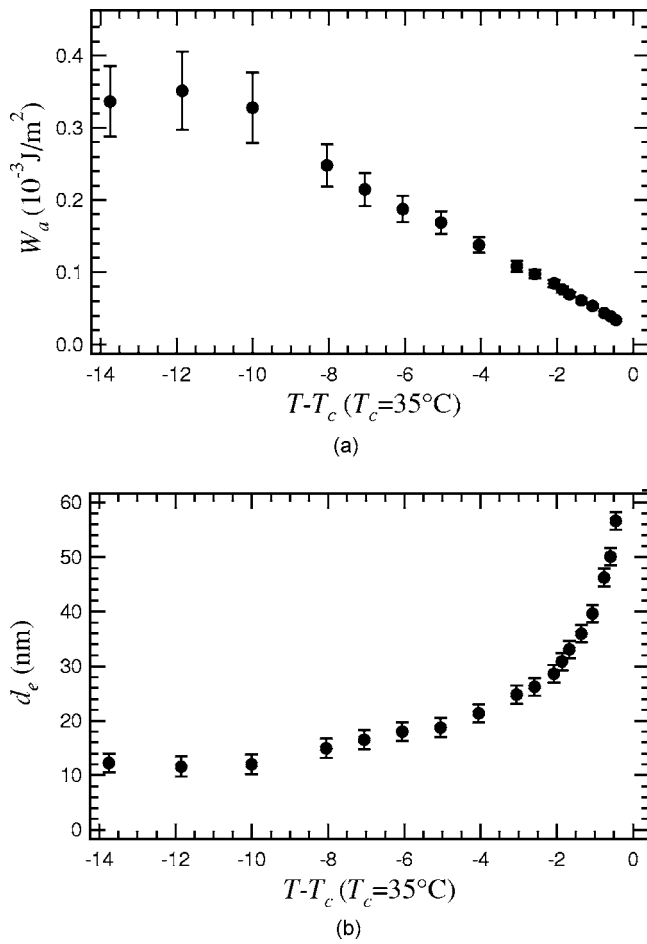


FIG. 8. (a) Azimuthal anchoring energy at the polyimide-5CB interface versus the reduced temperature. (b) Extrapolation length at the polyimide-5CB interface versus the reduced temperature.

and an extraordinary beam. It has been shown that the amplitudes of both these beams oscillate at the angular frequency 2ω . The phase coefficients are related to the surface azimuthal angle of the director and to the characteristic length of the twist bulk director distortion. In our experimental geometry, the spurious contribution due to the interfacial director twist is somewhat small and is quadratic in the amplitude of the electric field. On the contrary, the phase change due to the surface director rotation induced by the switching on of the electric field E is proportional to E . Thus, the two contributions can be easily separated by a proper fitting procedure. The anchoring energies measured here with the transmitted light method are consistent with those obtained by the reflected light method. However, the accuracy and the repeatability of these latter experimental results are much lower. In particular, the anchoring energies measured with the transmitted light method using the extraordinary ray or the ordinary ray can differ the one from the other up to 30%. A still greater difference is found as far as the quadratic contributions due to the director twist are concerned. For more details on the transmitted light results we refer the reader to Ref. [34]. These observed differences between ordinary and extraordinary transmitted beams are not predicted by the theory developed in [11] and will be the object of

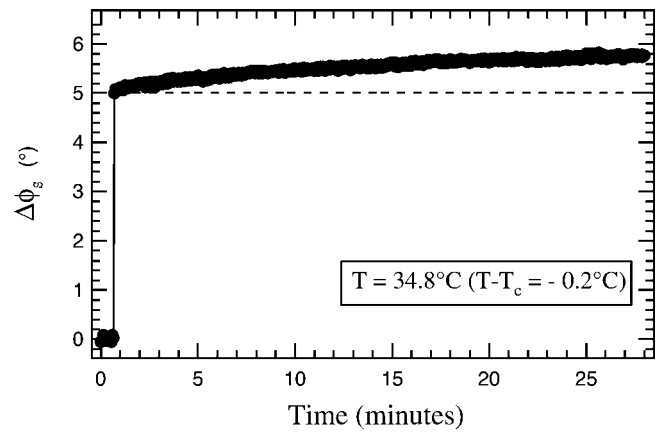


FIG. 9. Time response of the surface azimuthal director angle at the switching on of an electric field $E=0.29 \text{ V}/\mu\text{m}$ at the reduced temperature $T_r=T-T_c=-0.2 \text{ }^\circ\text{C}$. The electric field is switched on at time $t=42 \text{ s}$. After a first fast response time ($<1 \text{ s}$), the azimuthal angle shows a very slow drift due to a gliding of the easy axis.

further experimental and theoretical investigations. In conclusion, these latter experimental results with transmitted light confirm that the azimuthal anchoring at our nematic-polyimide interface is strong and demonstrate also that the reflectometric method remains actually the most accurate technique for strong anchoring energies measurements. The very high value of the measured azimuthal anchoring energy could be surprising, however it has to be emphasized that the experimental values of the azimuthal anchoring energy coefficients measured in the present experiment are comparable with those that have been recently reported in the literature [10,35] for similar polyimide rubbed substrates purchased by EHC. In these latter experiments the anchoring energy was measured using high accuracy transmitted light techniques. On the other hand, it has to be noted that our values of the azimuthal anchoring energy are much higher than the experimental values reported in references [6,36,37] for polyimide-nematic interfaces. Unfortunately, the value of the rubbing strength was not reported in the references [6,36,37] and, thus, a detailed comparison with our experimental results is not possible here. In fact, some experimental results [28] indicate that the anchoring energy depends greatly on the rubbing strength parameter L . In particular, in the case of the PVA-nematic interface, Sato *et al.* [28] found that the extrapolation length d_e is inversely proportional to the rubbing strength L in the measurement range $0 < L < 0.9 \text{ m}$. At the maximum value of L ($L \approx 0.90 \text{ m}$) they found $d_e \approx 80 \text{ nm}$. In our experiment, the rubbing strength is somewhat high ($L \approx 5 \text{ m}$) and this feature is consistent with a small value of the extrapolation length.

The time response of the surface director angle to a step-wise electric field is characterized by a fast initial response followed by a very slow relaxation. Figure 9 shows a typical time response of the surface director angle to the electric field. The electric field is switched on at time $t=42 \text{ s}$. A systematic investigation of the slow relaxation regime is not possible due to the presence of some thermal drift in the experimental signals which is superimposed to the actual director relaxation. Indeed, due to the presence of a strong

anchoring, the slow relaxation of the director at the surface is characterized by a small amplitude. Therefore, a small thermal drift affects appreciably the observed slow dynamics. Note that an analogous slow dynamics has been recently observed by other authors on rubbed polyimide substrates purchased by EHC and giving a strong azimuthal anchoring [35]. Finally, it has to be noticed that a similar behavior was recently observed [27] for the time response of the zenithal surface director angle at the same polyimide substrate used in our experiment. Therefore, the slow surface dynamic regime characterizes both the azimuthal and the zenithal relaxation of the director at the surface.

A similar slow dynamics of the surface azimuthal angle is currently observed in the case of weak azimuthal anchoring [20–26]. In such a case, it has been demonstrated [26] that the fast response time is virtually coincident with the characteristic bulk director reorientation time in the electric field. After this short characteristic time, the surface director angle reaches the quasistationary equilibrium condition where the equilibrium surface elastic torque is balanced by the restoring anchoring torque [see Eq. (4)]. With the typical electric fields used in our experiment, this fast response time is lower than 1 s. On the contrary, the slow dynamics is related to a gliding of the easy axis toward the direction of the electric field. This relaxation is characterized by a strongly nonexponential behavior and is well represented by a stretched exponential [19,26] or a power law [25]. The physical origin of the gliding is still object of investigation. This phenomenon is usually explained with the anisotropic adsorption desorption of nematic molecules from the interface (see, for instance, Ref. [38] and references therein). However, in the case of polymeric substrates, also a slow rotation of the surface polymeric chains due to the applied surface elastic torque could play some role [25]. We emphasize that observation of both a zenithal and an azimuthal gliding of the easy axis in the case of a strong anchoring energy demonstrates that the gliding phenomenon is a very general phenomenon that characterizes any kind of interface. In fact, we have always observed this typical slow dynamics in all our previous experiment with a lot of different substrates (PVA, glasses, SiO, PVCN, ...) having weak or moderately strong anchoring energies.

IV. CONCLUSIVE REMARKS

In this paper, we have measured the azimuthal anchoring energy at the interface between a rubbed polyimide layer and the NLC 5CB using a recently proposed high accuracy reflectometric method. A strong azimuthal anchoring is found at room temperature ($W_a=0.33 \times 10^{-3} \text{ J/m}^2$). Due to the smallness of the surface director rotation induced by the applied electric field, a great care has been devoted to control the many possible sources of spurious signals that could affect appreciably the experimental results. Furthermore, we have also performed some measurements using a high accuracy transmitted light technique that was recently proposed. Although the experimental results obtained with this latter method are affected by a much higher uncertainty and show a minor repeatability, they are consistent with the reflectometric results. The anchoring energy is found to be uniform on the whole polyimide layer and to decrease greatly as the clearing temperature of the NLC is approached.

The dynamic response of the surface director azimuthal angle to the external electric field exhibits the typical slow dynamic regime (*gliding* of the easy axis) which is usually observed in the case of weak anchoring substrates. This result agrees with very recent experimental results obtained by other authors for the azimuthal director angle at a similar polyimide interface [35]. The same behavior was recently observed on the same polyimide substrate as far as the zenithal surface director angle is concerned [27]. All these results demonstrate that the gliding of the easy axis at a nematic interface is a very general phenomenon which is not only related to weak anchoring substrates but characterizes any kind of interface.

ACKNOWLEDGMENTS

Many thanks to S. Joly and I. Dozov of NEMOPTIC for supplying us with the rubbed polyimide glass plates and for a careful reading of the manuscript. We acknowledge the Ministero dell' Istruzione, dell'Università e della Ricerca of Italy (MIUR) for financial support (PRIN 2004:2004024508003).

-
- [1] P. G. de Gennes, *The Physics of Liquid Crystals* (Clarendon, Oxford, 1974).
- [2] S. Faetti, *Physics of Liquid Crystalline Materials*, edited by I. C. Khoo and F. Simoni (Gordon and Breach Science Publishers, Philadelphia, 1991).
- [3] J. Sicart, *J. Phys. (France) Lett.* **37**, L25 (1976).
- [4] H. A. van Sprang, *J. Phys. (Paris)* **44**, 421 (1983).
- [5] G. Barbero, E. Miraldi, C. Oldano, M. L. Rastrello, and P. T. Valabrega, *J. Phys. (Paris)* **47**, 1411 (1986).
- [6] T. Oh Ide, S. Kuniyasu, and S. Kobayashi, *Mol. Cryst. Liq. Cryst.* **164**, 91 (1988).
- [7] S. Faetti and C. Lazzari, *J. Appl. Phys.* **71**, 3204 (1992).
- [8] E. Polossat and I. Dozov, *Mol. Cryst. Liq. Cryst. Sci. Technol.*, Sect. A **282**, 223 (1996).
- [9] I. Gerus, A. Glushenko, S. B. Kwon, V. Reshetnyak, and Y. Reznikov, *Liq. Cryst.* **28**, 1709 (2003).
- [10] S. Faetti, *Mol. Cryst. Liq. Cryst. Suppl. Ser.* **421**, 225 (2004).
- [11] S. Faetti and G. C. Mutinati, *Phys. Rev. E* **68**, 026601 (2003).
- [12] S. Faetti, V. Palleschi, and A. Schirone, *Nuovo Cimento D* **10**, 1313 (1988).
- [13] S. Faetti, M. Nobili, and A. Schirone, *Liq. Cryst.* **10**, 95 (1991).
- [14] S. Faetti and M. Nobili, *Liq. Cryst.* **25**, 487 (1998).
- [15] S. Faetti and G. C. Mutinati, *Eur. Phys. J. E* **10**, 265 (2003).
- [16] F. Z. Yang, H. E. Chey, and J. R. Sambles, *J. Opt. Soc. Am. B* **18**, 994 (2001).

- [17] F. Z. Yang, H. J. Gao, and J. R. Sambles, *J. Appl. Phys.* **92**, 1744 (2002).
- [18] M. Nobili, C. Lazzari, A. Schirone, and S. Faetti, *Mol. Cryst. Liq. Cryst. Sci. Technol., Sect. A* **212**, 97 (1992).
- [19] I. Gerus, S. Faetti, and G. C. Mutinati, *Mol. Cryst. Liq. Cryst. Suppl. Ser.* **421**, 81 (2004).
- [20] R. Barberi, I. Dozov, M. Giocondo, M. Iovane, P. Martinot Lagarde, D. Stoenescu, S. Tonchev, and L. V. Tsonev, *Eur. Phys. J. B* **44**, 83 (1998).
- [21] E. A. Oliveira, A. M. Figueiredo Neto, and G. Durand, *Phys. Rev. A* **44**, R825 (1991).
- [22] T. Nose, S. Masuda, and S. Sato, *Jpn. J. Appl. Phys., Part 1* **30**, 3450 (1991).
- [23] P. Vetter, Y. Ohmura, and T. Uchida, *Jpn. J. Appl. Phys., Part 1* **32**, 1239 (1993).
- [24] V. P. Vorflusev, H. S. Kitzerow, and V. G. Chigrinov, *Appl. Phys. Lett.* **70**, 3359 (1997).
- [25] I. Janossy and T. I. Kosa, *Phys. Rev. E* **70**, 052701 (2004).
- [26] S. Faetti, M. Nobili, and I. Raggi, *Eur. Phys. J. B* **11**, 445 (1999).
- [27] S. Joly, K. Antonova, P. Martinot-Lagarde, and I. Dozov, *Phys. Rev. E* **70**, 050701(R) (2004).
- [28] Y. Sato, K. Sato, and T. Uchida, *Jpn. J. Appl. Phys., Part 2* **31**, L579 (1992).
- [29] N. A. J. M. van Aerle, M. Barmantlo, and R. W. J. Hallering, *J. Appl. Phys.* **74**, 3111 (1993).
- [30] G. Bruhat, *Cours de Physique Generale: Optique* (Masson & C^{ie} Editions, Paris, 1965).
- [31] P. P. Karat and N. V. Madhusudana, *Mol. Cryst. Liq. Cryst.* **35**, 51 (1976).
- [32] T. Toyooka, G. Chen, H. Takezoe, and A. Fukuda, *Jpn. J. Appl. Phys., Part 1* **26**, 1959 (1987).
- [33] A. Bogi and S. Faetti, *Liq. Cryst.* **28**, 729 (2001).
- [34] P. Marianelli, thesis, University of Pisa, 2005.
- [35] I. Janossy (unpublished).
- [36] M. Vilfan and M. Copic, *Phys. Rev. E* **68**, 031704 (2003).
- [37] B. Zhang, P. Sheng, and H. S. Kwok, *Phys. Rev. E* **67**, 041713 (2003).
- [38] A. Romanenko, I. Pinkevich, V. Reshetnyak, I. Dozov, and D. Stoenescu, *Mol. Cryst. Liq. Cryst. Suppl. Ser.* **422**, 173 (2004).